



Resistance of surface nanostructures and ultrafine grain structures on steel 40Kh to wear and cavitation-erosive destruction

Yaroslav Kyryliv¹ · Volodymyr Kyryliv² · Bogdan Tsizh^{3,4} · Olha Maksymiv²

Received: 31 December 2020 / Accepted: 12 February 2021 / Published online: 2 March 2021
© King Abdulaziz City for Science and Technology 2021

Abstract

Wear resistance in oil and in conditions of dry friction, as well as resistance to cavitation-erosion destruction (CED) of samples made of steel 40Kh with a surface nanocrystalline and ultrafine grain structure formed by severe plastic deformation (SPD) by mechanical-pulse treatment (MPT) and vibration-centrifugal hardening (VCH) were studied. At the same time, for almost the same microhardness obtained by MPT, VCH forms a significantly greater thickness of the hardened layer, which makes it possible to carry out finishing operations for high-precision parts. It is shown that nanostructures and UFGS on steel 40Kh significantly reduced the friction coefficients of the test pair and its wear resistance under dry friction, as well as in oil, compared with quenching and low tempering, which is especially manifested in an oil medium by more than 2 times. It was conducted comparative studies of the stability of CED and revealed their correlation with wear resistance. At the same time, the resistance to CED depends on the processing modes, which form favorable electrochemical characteristics of the hardened surface layer.

Keywords Nanocrystalline structure · Ultrafine grain structure · Mechanical-pulse treatment · Vibration-centrifugal hardening · Wear resistance · Cavitation-erosion destruction

Introduction

One of the main directions of modern materials science is the development of methods for obtaining and studying the properties of fine and nanocrystalline structures (NCS). SPD

is the most widespread method of NCS formation (Valiev et al. 2016; Ensafi et al. 2017; He et al. 2015). This method is used to form volumetric (Valiev et al. 2016; Ensafi et al. 2017; He et al. 2015; Zhao et al. 2018) and surface (Bagheri et al. 2015) NCS. The formation of surface NCS is technologically simpler and therefore more common. This method is used to obtain NCS and UFGS. The technology of MPT with high-speed friction as the generator of the SPD is well-known (Nykyforchyn et al. 2014). It forms a surface NCS, which increases surface microhardness, wear resistance (Kyryliv 2012), fatigue (Kyryliv et al. 2018a) and contact fatigue (Kyryliv et al. 2016). A well-known method of forming UFGS is VCH (Kyryliv et al. 2018b). Its feature is to apply significant forces to the surface through the balls fixed in a special cage, which leads to an increase in the contact stresses in the processing zone and, accordingly, to an increase in depth (up to 6 mm) and microhardness of the hardened surface layer. In particular, this treatment can be used to strengthen high-precision cylindrical surfaces, since the significant depth of hardening allows finishing operations.

✉ Yaroslav Kyryliv
yaroslav_kyryliv@ukr.net

Volodymyr Kyryliv
kyryliv@ipm.lviv.ua

Bogdan Tsizh
tsizhb@ukr.net

Olha Maksymiv
okyryliv@yahoo.com

¹ Lviv State University of Life Safety, 35 Kleparivska St., Lviv 79007, Ukraine

² Karpenko Physical-Mechanical Institute of the NAS of Ukraine, 5 Naukova St., Lviv 79060, Ukraine

³ Kazimierz Wielki University in Bydgoszcz, 30 Chodkiewicza St., 85-064 Bydgoszcz, Poland

⁴ Stepan Gzhytskyi National University of Veterinary Medicine and Biotechnologies, 50 Pekarska St., Lviv 79010, Ukraine

The aim of the work is to carry out comparative studies of wear resistance in oil and dry friction and resistance to CED of steel 40Kh processed by those methods.

Materials and methods

The MPT of samples from steel 40Kh (0.4C–1Cr) for research was carried out on a setup (Kalichak et al. 1989) (Fig. 1a) under the following modes: the linear velocity of a reinforced tool made of steel 40Kh–60 m/s, the rotation frequency of the samples is 0.33 s^{-1} , the longitudinal feed of the tool along the sample is $1.9 \times 10^{-4} \text{ m/rad}$. Carrying out MPT, mineral oil I-12A with the addition of low molecular weight polyethylene was used as a technological cooling medium (Kyryliv 1999). VCH (Kyryliv et al. 2018b) of samples from the same steel was carried out on a special vibration-centrifugal hardening installation (Fig. 1b) under the following modes: vibration amplitude $A = 5 \text{ mm}$; vibration frequency $f = 24 \text{ Hz}$; working tool mass $m = 4.5 \text{ kg}$ (samples for the study of wear resistance), 7.5 kg (for corrosion and erosion tests); processing time $\tau = 1680 \text{ s}$; eccentricity $\varepsilon = 10 \text{ mm}$. A different mass of the tool was chosen taking into account the fact that at $m = 4.5 \text{ kg}$, we obtained the maximum microhardness of

the hardened layer (Kyryliv et al. , b), and at $m = 7.5 \text{ kg}$ —favorable electrochemical characteristics of the surface material for corrosion-erosion studies (Kyryliv et al. 2019).

To determine the microhardness and depth of the hardened layer of treated samples, PMT-3 microhardness tester was used. Tests were carried out by indentation of a standard 136-degree Vickers diamond pyramid indenter with a square base at a load of 0.1 kg . Microhardness was determined by the formula:

$$H_{\mu} = \frac{1854P}{d^2},$$

where P is the load and d is the diagonal of the square print.

The phase composition of the steel surface after hardening treatments was investigated on a DRON-3 diffractometer–diffractograph in $\text{CuK}\alpha$ radiation ($U = 30 \text{ kV}$, $I = 20 \text{ mA}$) with a step of $8.75 \times 10^{-4} \text{ rad}$ and exposure at point 4 s. For those studies and CED samples were made in the form of sectors with an arc length of 14 mm . Diffraction patterns were processed using the CSD software (Kraus and Nolze 1996). X-ray diffraction patterns were identified using the JCPDS-ASTM file (Powder 1974).

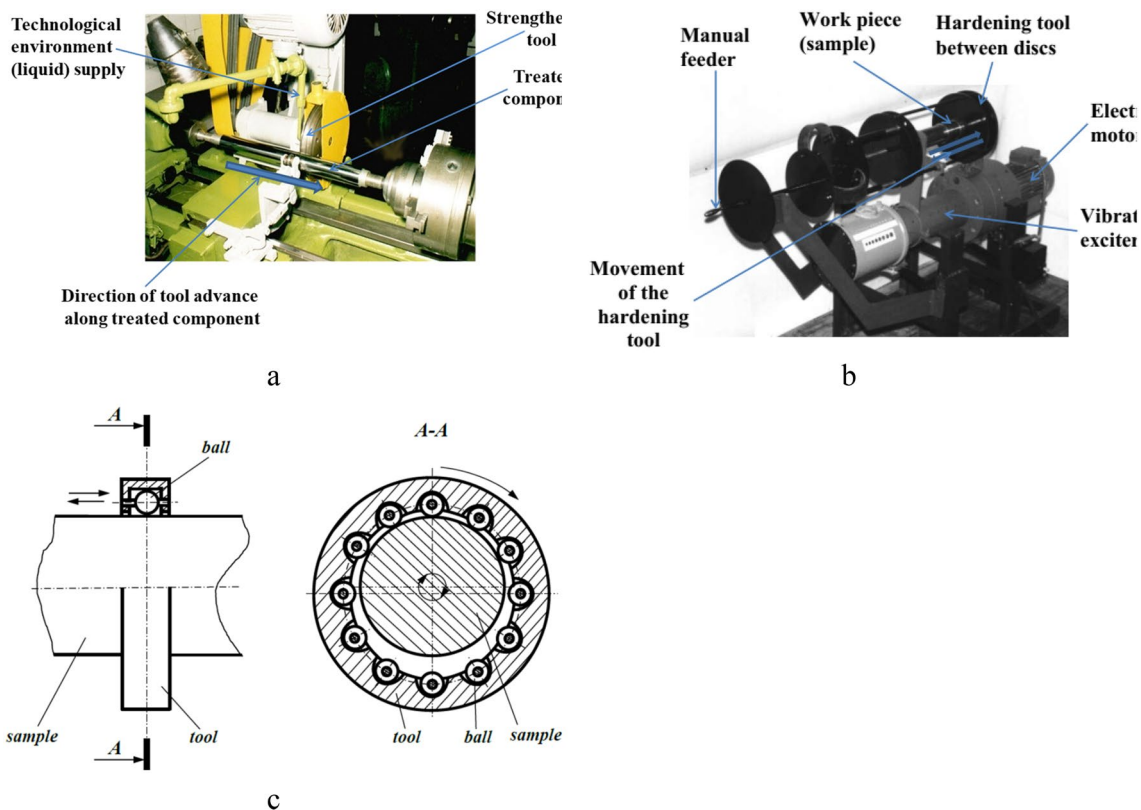


Fig. 1 Installations for MPT (a), VCH (b) and a schematic representation of the VCH process (c)

The study of wear resistance was carried out according to the ring-insert scheme on a MI-1 M friction machine. Cylindrical annular samples were made of steel 40Kh after normalization with an outer diameter of 75, a width of 12 and a thickness of 6 mm and processed with VCH. The study of wear resistance after MPT was carried out on annular samples with a diameter of 75 and a width of 10 mm. To study the wear resistance, the rings were fixed in a special mandrel. For study of effect of both treatments, we used inserts made of high-strength cast iron VCh60 (3.3C–2.6Si–0.6Mn–0.3Ni–0.1Cr) with a load of 2 MPa. Sample rings for the study of wear resistance were tested after MPT without additional operations, and after VCH and heat treatment, they were ground to the same roughness as the samples after MPT ($R_a = 0.8 \mu\text{m}$). Both types of hardening were compared with samples after quenching and tempering at 200 °C.

CED was investigated in tap water of medium hardness (pH 6.3 ... 6.8, hardness 1.9 ... 2.05 mol/m³) by the magnetostrictive method according to the method (Nykyforchyn et al. 2002) with the bottom arrangement of the samples. The gap between the end of the magnetostrictor emitter and the sample is 0.5 mm. Samples for cavitation tests were made with rectangular dimensions 14 × 12 mm and a thickness of 3 mm. Cavitation loads were created with an amplitude of $A = 70 \mu\text{m}$ by a magnetostrictive transducer. Stabilized CED rate and incubation period were taken as destruction parameters.

Erosion losses were measured gravimetrically. The samples under study for cavitation erosion before and after tests were washed in acetone, then in ethyl alcohol, after which they were dried, and only after that they were weighed on an analytical balance VLA-200 M (Kyryliv et al. 2019) with an accuracy of $\pm 0.0001 \text{ g}$. Weighing of test samples for wear resistance was carried out on the same balance.

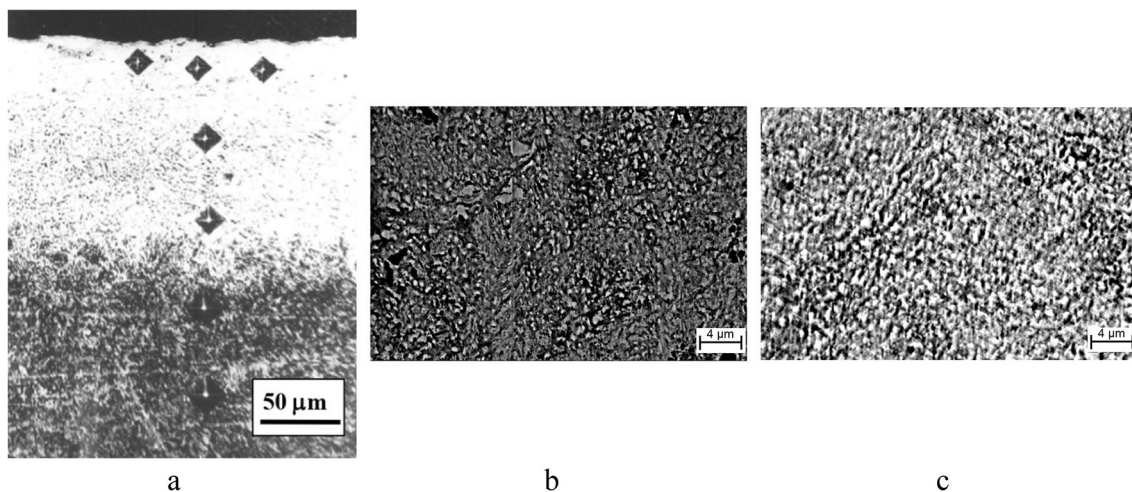


Fig. 2 The microstructure of steel 40Kh after: **a** MPT surface layer, **b** VCH at depths 100 μm , **c** matrix structure after VCH at depth 6 mm

Results and discussion

Metallographic studies of the cross section of the sample after MPT in depth from the surface revealed a hardened surface layer in the form of an un-etched area (so called “white layer”) (Fig. 2a). It can be seen visually that the dimensions of microhardness imprints in the hardened layer were smaller than in the matrix material, which indicates its high microhardness. The distribution of microhardness H_{μ} along the depth δ from the surface (Fig. 3) showed that it varied from a maximum value of about 9.4 on the surface to 2.2 GPa in the matrix material, which was 4 times less. The thickness of the hardened layer was about 150 μm and corresponded to the thickness of the non-etched area revealed by metallographic analysis. This correspondence showed a high microhardness of the surface layer obtained due to the fragmentation of the structure to nanosize.

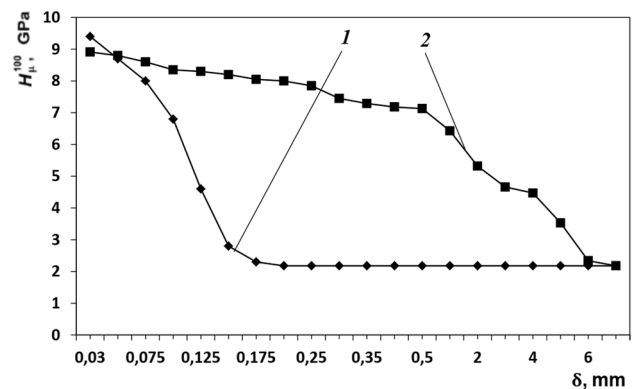


Fig. 3 Microhardness of the hardened layers of steel 40Kh after various treatments: 1–MPT; 2–VCH

After VCH, the microstructure is strongly fragmented near the surface at a depth of 100 μm (Fig. 2b). The grains are broken into separate blocks in some places unevenly. At a depth of 1000 μm , the microstructure is similar, and the grain size distribution decreases, apparently, due to a more uniform distribution of deformation upon impact of the balls' surfaces, and smoothly passes to the initial matrix structure (Fig. 2c). Under the optimal processing conditions of VCH: $m=4.5$ kg; $\tau=1680$ s, the obtained hardening depth $\delta=6$ mm and microhardness from 8.9 to 2.3 GPa (Fig. 3). It is known that normalized steel 40Kh has a ferritic-perlite structure, which has an α -phase and Fe_3C . After SPD of steel with the above treatments, we obtain only a ferritic fine-crystalline structure, which is confirmed by X-ray studies (Fig. 4). This is explained by the fact that during the SPD, namely under the action of high pressure in the friction contact zone, the decomposition of cementite occurs with the “extraction” of carbon at the grain boundaries. The process of “extraction” carbon from the cementite lattice is possible, because the binding energy of carbon atoms in the cementite lattice is 0.064–0.067 aJ less than the binding energy of dislocations with carbon atoms (0.128 aJ) (Gavrilyuk 2003). The kinetics of the “extraction” process is due to the accelerated transfer by plastic deformation of carbon atoms from cementite in the field of action of ferrite dislocations (Firstov et al. 2006). Saturation of the boundaries with impurity carbon atoms increases their local density, increases the hardness of the material with NCS, and inhibits recrystallization processes (Firstov et al. 2006). The grain boundary distribution of carbon in armco-iron after MPT with surface carbon saturation was also confirmed in (Nykyforchyn et al. 2014) analysis of Fisher concentration curves obtained by layer-by-layer chemical analysis. After MPT, the grain size on the surface is ~ 60 nm and after VCH–190 nm. The main increase in microhardness was obtained due to

refinement of the structure, its high defectiveness (dislocation density after MPT and VCH achieved $4.3 \times 10^{12} \text{ cm}^{-2}$ and $1.3 \times 10^{12} \text{ cm}^{-2}$, respectively) and high stresses in the lattice after MPT–0.036 and VCH–0.106%.

The wear resistance of friction pairs in the processing of rings by two methods of hardening (Fig. 5, columns 1, 2) is higher compared to their quenching and tempering at 200 $^\circ\text{C}$ (Fig. 5, columns 3). The wear rate of friction pairs correlates well with the coefficients of friction: friction pairs after MPT have a low coefficient of friction–0.5, slightly higher–0.54 after VCH, and quenching with tempering at 200 $^\circ\text{C}$ is inferior to MPT and VCH and is 0.62. The difference in wear resistance of friction pairs after both treatments is insignificant. So, in conditions of dry friction of high-precision parts (below the accuracy class 9 ... 10) (ISO 2010 ISO 286-2), VCH has an advantage over MPT due to the possibility

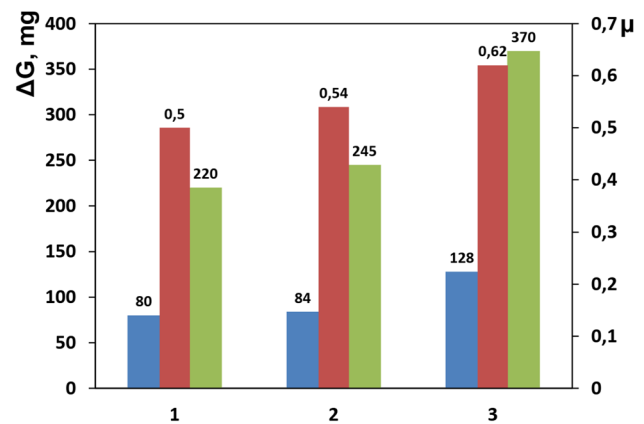


Fig. 5 Wear of friction pair steel 40Kh–VCh60 after various treatments: (Blue square—ring; Green square—insert) and coefficient of friction (Red square) after dry friction: 1–MPT; 2–VCH; 3–quenching with tempering at 200 $^\circ\text{C}$

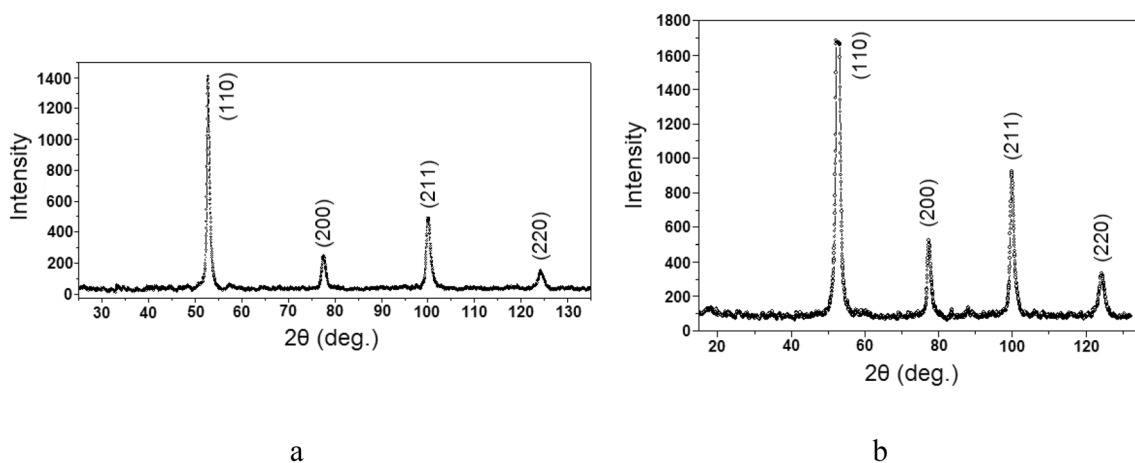


Fig. 4 The diffraction patterns of steel 40Kh after MPT (a) and VCH (b) at depths of 50 and 100 μm

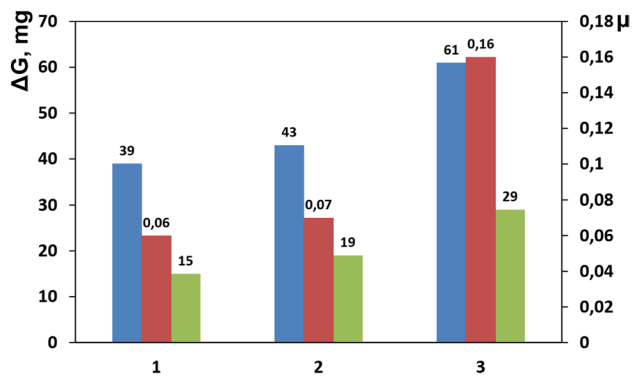


Fig. 6 Wear of friction pair steel 40Kh–VCh60 after various treatments: (Blue square—ring; Green square—insert) and coefficient of friction (Red square) in AS-8 oil: 1–MPT; 2–VCH; 3–quenching with tempering at 200 °C

of finishing operations, which ensures accuracy above the specified tolerance range. It is expected that in oil the wear resistance of all friction pairs will be higher (Fig. 6). Surface hardening by these methods (Fig. 6, columns 1, 2) has more than 2 times higher wear resistance compared to heat treatment (Fig. 6, column 3), which is associated with a significant reduction in the coefficient of friction to 0.06 and 0.07 for MPT and VCH, respectively (Fig. 6), which is typical for nano- (Kyrlyiv 2012) and ultrafine grain (Kyrlyiv et al. 2018b) structures. The significant decrease in the friction coefficient of nanostructured surfaces is explained (Buckleu 1981) by the change in the deposition of d-orbital electrons on the metal bond due to the effect of SPD on the metal. An increase in the interatomic interaction inside the metal leads to its decrease on the surface. For nanostructures, this is caused by high pressure during SPD treatment, which are transformed into large lattice distortions, high dislocation densities, and residual compressive stresses in the surface layers. Lower coefficients of friction of hardened surfaces in oil compared to dry friction reduce the temperature in the frictional contact zone, thereby reducing the possible destruction of the lubricating layer and the loss of its lubricating ability. (Mikosyanchyk et al. 2019, Laber and Laber 2015). The increase in wear resistance is also associated with the improvement of the micromechanical characteristics of the surface layer after hardening (Holubets' et al. 2019; Chen et al. 2020).

The characteristics of the CED-stability of steel 40Kh after various technological processing methods differ significantly (Fig. 7). According to the criterion of the stabilized CED speed W_{st} (Fig. 7), the MPT and VCH turned out to be the most effective at $m=7.5$ kg, $\tau=1680$ s and a test amplitude of 70 μm . Since CED is believed to arise by the micro-fatigue mechanism, the presence of an inhomogeneous surface with significant defects in the corrosive surface greatly facilitates the destruction of the material. This is due to the relatively

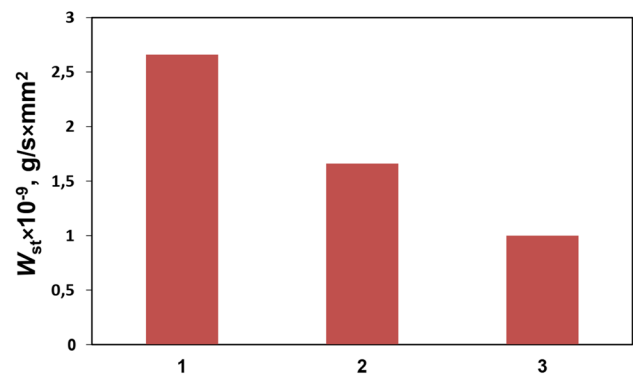


Fig. 7 The dependence of the stabilized speed of CED on the amplitude of testing 70 μm of samples of steel 40Kh after various treatments: 1–quenching with tempering at 200 °C; 2–VCH ($m=7.5$ kg, $\tau=1680$ s); 3–MPT

insignificant microhardness of the hardened layer in comparison with the depth of the CED effect (Fig. 7, column 1). So, the MPT and VCH technologies increase the durability of machine parts operating under CED conditions. More effective for VCH are modes that are characterized by a slightly lower microhardness, but have a higher corrosion resistance. An increase in the resistance of CED is also associated with an increase in the polarization resistance of steel after MPT (Nykyforchyn et al. 2002) and VCH (Kyrlyiv et al. 2019) to 14 and 9.6 $\text{k}\Omega/\text{cm}^2$, respectively, and a shift in the corrosion potential to positive values. The cavitation-erosion resistance in terms of the stabilized CED rate increases 1.6 times compared to the hardened and tempered at 200 °C (Fig. 7). MPT under the same conditions provides an increase in resistance to CED by 2.6 times.

Conclusions

1. The MPT technology provides the formation of a NCS, and the VCH forms an UFGS. The microhardness of the NCS is somewhat higher than that of UFGS.
2. After VCH, the depth of the hardened layer is much greater, which makes it possible to carry out finishing operations for high-precision parts.
3. Both methods provide high wear resistance and resistance to CED in comparison with traditional heat treatment, which is associated with high surface hardness, reduced friction coefficients and favorable electrochemical characteristics.

Declarations

Conflict of interest The authors declare that there is no conflict of interest.

References

- Bagheri H, Gheyhani M, Masiha H et al (2015) Nanocrystallization by surface mechanical attrition treatment. In: Aliofkhaezraei M (ed) Handbook of mechanical nanostructuring. Wiley, Verlag, pp 325–377
- Buckleu DH (1981) Surface effects in adhesion, friction, wear, and lubrication. Elsevier, Amsterdam, Oxford, New York
- Chen X, Han Z, Li XY, Lu K (2020) Friction of stable gradient nano-grained metals. *Scripta Mater* 185:82–87. <https://doi.org/10.1016/j.scriptamat.2020.04.041>
- Ensafi M, Faraji G, Abdolvand H (2017) Cyclic extrusion compression angular pressing (CECAP) as a novel severe plastic deformation method for producing bulk ultrafine grained metals. *Mat Lett* 197:12–16. <https://doi.org/10.1016/j.matlet.2017.03.142>
- Firstov SO, Rohul TH, Svechnikov VL et al (2006) Concept of “useful” impurities and mechanical properties of nanostructured chromium and molybdenum films. *Mater Sci* 42(1):121–126. <https://doi.org/10.1007/s11003-006-0064-y>
- Gavrilyuk VG (2003) Decomposition of cementite in perlitic steel due to plastic deformation. *Mater Sci Eng A* 345(1–2):81–89. [https://doi.org/10.1016/S0921-5093\(02\)00358-1](https://doi.org/10.1016/S0921-5093(02)00358-1)
- He Y, Li K, Cho IS et al (2015) Microstructural characterization of SS304 upon various shot peening treatments. *Appl Microsc* 45(3):155–169. <https://doi.org/10.9729/AM.2015.45.3.155>
- Holubets VM, Pashechko MI, Borc J et al (2019) Micromechanical characteristics of the surface layer of 45 steel after electric-spark treatment. *Mater Sci* 55:409–416. <https://doi.org/10.1007/s11003-019-00318-8>
- ISO 2010 ISO 286-2 Geometrical product specifications (GPS)—ISO code system for tolerances on linear sizes—part 2: tables of standard tolerance classes and limit deviations for holes and shafts
- Kalichak TN, Kyryliv VI, Fenchny SV (1989) Mechanopulsed hardening of long component of the hydraulic cylinder rod type. *Mater Sci* 25(1):96–99. <https://doi.org/10.1007/BF00727938>
- Kraus W, Nolze G (1996) Powder cell—a program for the representation and manipulation of crystal structures and calculation the resulting X-ray powder patterns. *J Appl Cryst* 29:301–303. <https://doi.org/10.1107/S0021889895014920>
- Kyryliv V (1999) Surface saturation of steel with carbon during mechanical-pulse treatment. *Mater Sci* 35(6):853–8594. <https://doi.org/10.1007/BF02359467>
- Kyryliv VI (2012) Improvement of the wear resistance of medium-carbon steel by nanodispersion of surface layers. *Mater Sci* 48(1):119–123. <https://doi.org/10.1007/s11003-012-9481-2>
- Kyryliv VI, Chajkovs'kyj BP, Maksymiv OV et al (2016) Contact fatigue of 20KHN3A steel with surface nanostructure. *Mater Sci* 51(6):833–838. <https://doi.org/10.1007/s11003-016-9909-1>
- Kyryliv VI, Chajkovs'kyj BP, Maksymiv OV et al (2018a) Fatigue and corrosion fatigue of the roll steels with surface nanostructure. *J Nano Res* 51:92–97
- Kyryliv V, Kyryliv Y, Sas N (2018b) Formation of surface ultrafine grain structure and their physical and mechanical characteristics using vibration-centrifugal hardening. *Adv Mater Sci Eng*. <https://doi.org/10.1155/2018/3152170>
- Kyryliv Y, Kyryliv V, Sas N (2019) Influence of surface ultrafine grain structure on cavitation erosion damage resistance. In: Fesenko O, Yatsenko L (eds) *Nanocomposites, nanostructures, and their applications*. Springer, Cham, pp 97–107
- Laber S, Laber A (2015) Modifying operating conditions of the friction couple with an additive added to the lubricant while operating. *Solid State Phenom* 220–221:230–238
- Mikosyanchyk OO, Mnatsakanov RH, Lopata LA et al (2019) Wear resistance of 30KhGSA steel under the conditions of rolling with sliding. *Mater Sci* 55:402–408. <https://doi.org/10.1007/s11003-019-00317-9>
- Nykyforchyn HM, Kyryliv VI, Bassarab AI et al (2002) Wear resistance of mechanical-pulse treated 40Kh steel during abrasive friction and cavitation. *Mater Sci* 38:873–879. <https://doi.org/10.1023/A:1024272120417>
- Nykyforchyn H, Kyryliv V, Maksymiv O (2014) Physical and mechanical properties of surface nanocrystalline structures, generated by severe thermal-plastic deformation. In: Fesenko O, Yatsenko L (eds) *Nanocomposites, nanophotonics, nanobiotechnology, and applications*. Springer, Cham, pp 31–41
- Powder diffraction file search manual: alphabetical listing and search section of frequently encountered phases (1974) Philadelphia, JCPDS, p 839
- Valiev R, Estrin Y, Horita Z et al (2016) Fundamentals of superior properties in bulk nano SPD materials. *Mat Res Lett* 4:1–21. <https://doi.org/10.1080/21663831.2015.1060543>
- Zhao X, Zhao B, Liu Y et al (2018) Research on friction and wear behavior of gradient nano-structured 40Cr steel induced by high frequency impacting and rolling. *Eng Failure Analysis* 83:167–177. <https://doi.org/10.1016/j.engfailanal.2017.09.012>

Publisher's Note Springer Nature remains neutral with regard to jurisdictional claims in published maps and institutional affiliations.